RESEARCH ARTICLE | FEBRUARY 06 2023

Role of cationic size mismatch and effect of disorder in mixed valent manganites

Special Collection: 67th Annual Conference on Magnetism and Magnetic Materials

Aisha Khatun ; Payel Aich ; D. Topwal

AIP Advances 13, 025125 (2023)
https://doi.org/10.1063/9.0000526

Role of cationic size mismatch and effect of disorder in mixed valent manganites

Cite as: AIP Advances 13, 025125 (2023); doi: 10.1063/9.0000526
Submitted: 3 October 2022 • Accepted: 18 November 2022 •
Published Online: 6 February 2023

Aisha Khatun,[1,2] Payel Aich,[1,2] and D. Topwal[1,2,a)]

AFFILIATIONS

[1] Institute of Physics, Sachivalaya Marg, Bhubaneswar 751005, India
[2] Homi Bhabha National Institute, Training School Complex, Anushakti Nagar, Mumbai 400094, India

Note: This paper was presented at the 67th Annual Conference on Magnetism and Magnetic Materials.
[a)]**Author to whom correspondence should be addressed:** dinesh.topwal@iopb.res.in

ABSTRACT

Comparative studies of structure, magnetism, and magnetoresistance (MR) have been carried out in A-site ordered $NdBaMn_2O_6$ (O-NB), A-site disordered $NdBaMn_2O_6$ (D-NB) and *A*-site disordered $NdCaMn_2O_6$ (D-NC). O-NB, where *A*-site cations, Nd^{3+} and Ba^{2+} (of different ionic sizes) are arranged periodically, undergoes structural transition with temperature, while no structural change is present in D-NB where *A*-site cations are arranged randomly. However, structural transitions are observed in D-NC where Nd^{3+} and Ca^{2+} have similar ionic sizes. Magnetization (M) data shows O-NB has AFM ground state associated with a lower structurally symmetric phase and an FM ground state is observed for D-NB with higher structural symmetry. However, AFM ground state is observed in D-NC similar to that of O-NB. Both the disorder systems exhibit semiconductive transport characteristics over the entire temperature range. The resistivity data of disorder compounds have been fitted with different theoretical models to elucidate the conduction process in these systems. Further, MR studies depict a three times higher value of MR in both disorder compounds compared to that of order one. However, the behavior of MR with H is different for D-NB and D-NC, implying a different origin of this large MR in these compounds. We believe that the different magnetic ground state of D-NB and D-NC is the possible origin of their distinct MR behavior to the magnetic field.

I. INTRODUCTION

Perovskite manganites with the general formula $(R_{1-x}^{3+}R'_x{}^{2+})MnO_3$[1] have drawn a lot of attention in the scientific community due to their intriguing physical features, including colossal magnetoresistance (CMR), metal-insulator transition (MI), and ferromagnetic-antiferromagnetic transition (FM-AFM). Physical properties of these systems can be tuned by many thermodynamic variables (like temperature, pressure, magnetic field etc.) as well as non-thermodynamic variables like *A*-site disorder [random distribution between *A*-site elements, R^{3+} and R'^{2+}, in $(R_{1-x}^{3+}R'_x{}^{2+})MnO_3$]. Millange *et al.* first investigated the difference between the *A*-site ordered and *A*-site disordered $LaBaMn_2O_6$ and reported that the ground states of both materials are FM metal with different Curie temperatures.[2] Latter, Akahoshi *et al.* and Nakajima *el al.* reported that *A*-site disorder in $LnBaMn_2O_6$ (Ln^{3+}—rare earth ions) suppresses different long-range interactions and gives rise to colossal magnetoresistive effect.[3,4] The ground state of *A*-site disorder manganites is greatly influenced by the *A*-site cationic size differences. For example, *A*-site disordered $PrBaMn_2O_6$ ($r_{Pr3+} - r_{Ba2+} = 0.31$ Å) system has FM ground state[3] while an AFM ground state is observed in *A*-site disordered $PrSrMn_2O_6$ system[5] ($r_{Pr3+} - r_{Sr2+} = 0.14$ Å) where Pr^{3+} and Sr^{2+} have nearly similar ionic sizes. Such a great impact of *A*-site cationic size differences in controlling the ground states of the disorder systems has not been explored yet. This article studied the crucial role of *A*-site cationic disorder and their ionic size mismatch in controlling the physical properties of mixed valent manganites. For this purpose *A*-site ordered $NdBaMn_2O_6$ (O-NB), *A*-site disordered $NdBaMn_2O_6$ (D-NB) ($r_{Nd3+} - r_{Ba2+} = 0.34$ Å) and *A*-site disordered $NdCaMn_2O_6$ (D-NC) ($r_{Nd3+} - r_{Ca2+} = 0.07$ Å) samples have been synthesized by solid state reaction method.

The thermal stability of crystallographic phases of the compounds has been investigated using temperature dependent powder

X-ray diffraction (XRD) technique. Temperature variations of magnetization have been carried out to reveal the magnetic ground state of the compounds. Resistivity measurement has been done for the disorder samples and investigated using different analytical models to reveal different conduction mechanisms of the systems. Finally, magnetic field dependent magnetoresistance measurement has been carried out to explore the influence of magnetic ordering on the transport properties of the systems.

II. EXPERIMENTAL DETAILS

Polycrystalline samples of O-NB, D-NB and D-NC have been prepared by the solid-state reaction method. Stoichiometric amounts of Nd_2O_3, $BaCO_3/CaCO_3$, and Mn_2O_3 were mixed, ground, and calcined at 1000 °C for 12 h in a reduced atmosphere (Ar/H_2). The resulting powder was reground, pressed into pellets, and sintered at 1100–1350 °C in the same reduced atmosphere. Using these conditions, an oxygen-deficient perovskite was obtained. Thereafter, we annealed the sample at 350 °C in an oxygen atmosphere to remove the oxygen deficiency and get the required stoichiometric specimen.

Temperature dependent XRD measurements were carried out at P02.1 beam-line of PETRA III in DESY Synchrotron Centre, Germany, with the wavelength of 0.20736 Å.[6,7] XRD data were analyzed via Rietveld refinement using the FullProf program. Electrical resistivity measurements were carried out by a conventional four-probe method in a temperature range from 3 K to 380 K in Quantum design (QD) Physical properties measurement system (PPMS). Magnetization measurements were carried out at a fixed magnetic field of 100 Oe in a field cooled (FC) mode in a temperature range from 5 K to 320 K in a vibrating sample magnetometer (VSM) of QD-PPMS.

III. RESULTS AND DISCUSSIONS

In *A*-site ordered state of $RR'Mn_2O_6$ (R^{3+} = Nd^{3+}, R'^{2+} = Ba^{2+}/Ca^{2+}) system, the R^{3+} and R'^{2+} cations stuck alternatively along the *c*-axis, sandwiching the MnO_2 layer between RO and R′O layers (*ab* plane). However, in A-site disordered samples, MnO_2 lies between the (RR′)O layers where the cations are randomly distributed.[3] Figures 1(a)–(c) shows XRD patterns of O-NB, D-NB and D-NC respectively, measured at temperatures 340 K and 130 K. The XRD patterns reflect that a good number of fundamental Bragg peaks get splitted clearly with decreasing temperature for O-NB and D-NC compounds. However, no such change has been observed for D-NB compound.

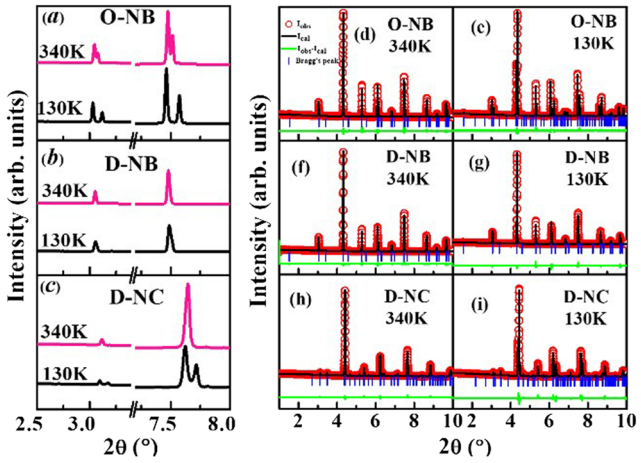

FIG. 1. (a)–(c) XRD pattern at T = 340 K and 130 K, (d)–(i) Rietveld refinement of the XRD patterns (open symbols—experimental data, black line—refined data, scatter line—Bragg peak, green line—difference between observed and calculated data).

Rietveld refinement of these XRD data [Figs. 1(d)–(i)] has been done to analyze the crystallographic phase of these compounds at different temperatures. The compound O-NB shows the crystallographic change from a higher symmetric tetragonal crystal structure (SG: *P*4/*mmm*) to a lower symmetric orthorhombic structure (SG: $P2_1am$) with decreasing the temperature. The occurrence of *A*-site disorder in the same system suppressed this structural change, such that the tetragonal crystal structure (SG: *P*4/*mmm*) persists at all temperatures for D-NB compound. Interestingly, despite having an *A*-site disorder, the crystal structure of the D-NC compound shows change from orthorhombic (SG: *Pnma*) to lower symmetric monoclinic (SG: *P*21/*m*) phase as temperature decreases. The obtained structural parameters are listed in Table I.

Figures 2(a)–(c) shows temperature variation of magnetization data of O-NB, D-NB, and D-NC compounds, respectively. The compound O-NB exhibits an AFM transition near 280 K [see Fig. 2(a)] accompanied by lower symmetric orthorhombic structural phase.[8] The A-site disorder suppresses the AFM interaction, such that the D-NB compound shows only FM transition near

TABLE I. Magnetic state (MS), crystal structure (CS), space group (SG), lattice constants (*a*, *b*, *c*) and average Mn-O-Mn bond angles (Θ) of O-NB, D-NB and D-NC at temperatures 340 K and 130 K are presented.

	T (K)	MS	CS	SG	*a* (Å)	*b* (Å)	*c* (Å)	Θ (°)
O-NB	130	AFM	Orthorombic	$P2_1am$	5.544 4(1)	5.546 9(1)	7.620 2(2)	165.0(3.0)
	340	PM	Tetragonal	*P*4/*mmm*	3.901 88(1)	3.901 88(1)	7.733 89(3)	177.5 (2.0)
D-NB	130	PM	Tetragonal	*P*4/*mmm*	3.893 19(1)	3.893 19(1)	7.747 74(5)	177.0(3.0)
	340	PM	Tetragonal	*P*4/*mmm*	3.897 25(1)	3.897 25(1)	7.772 49(3)	176.9(2.5)
D-NC	130	AFM	Monoclinic	*P*21/*m*	5.435 43(7)	7.494 14(7)	5.416 93(7)	153.0(2.0)
	340	PM	Orthorombic	*Pnma*	5.409 94(4)	7.604 00(5)	5.387 48(4)	157.9(1.0)

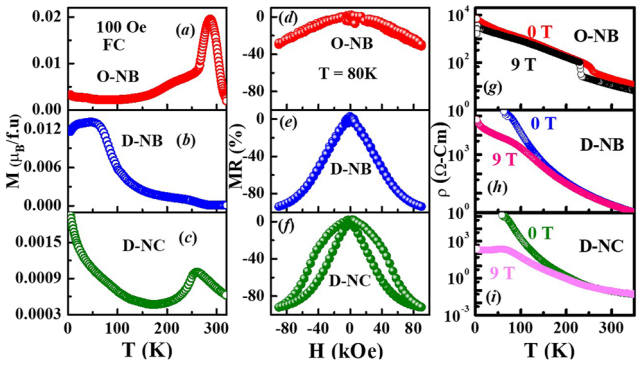

FIG. 2. Plot of (a)–(c) M vs T, (d)–(f) MR vs H and (g)–(i) ρ vs T of O-NB, D-NB and D-NC compounds respectively.

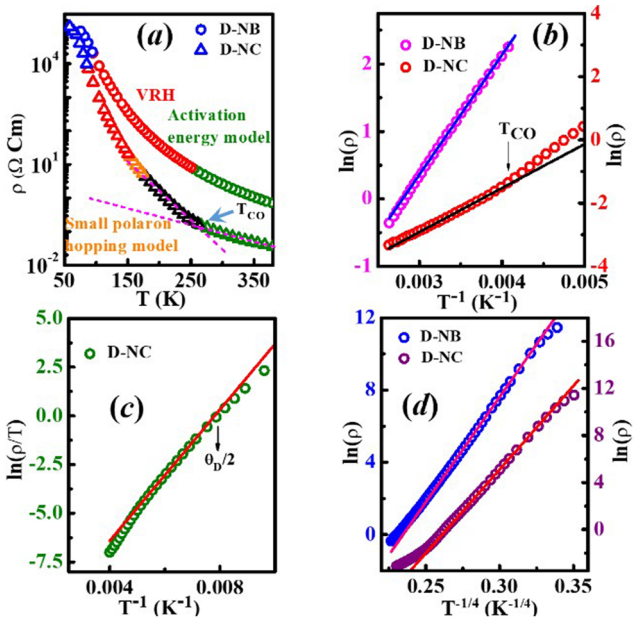

FIG. 3. Plot of (a) ρ vs T, (b) ln(ρ) vs T^{-1} (c) ln(ρ/T) vs T^{-1} (d) ln(ρ) vs $T^{-1/4}$ for D-NB and D-NC compounds.

76 K [see Fig. 2(b)] associated with a higher symmetric tetragonal structural phase. Interestingly, the D-NC compound shows AFM transition [see Fig. 2(c)] along with monoclinic structural phase[9,10] below 260 K.

The magnetic states and some of the refined structural parameters are summarized in Table I for all three compounds. Interesting quantities in these crystal structures are average Mn-O-Mn bond angles which are listed in the column Θ. At 130 K, the Mn-O-Mn bond angles are ~165° and 153° for O-NB and D-NC, respectively and the corresponding bond angle for D-NB compound is ~177°. So, the Mn-O-Mn bond angles in O-NB and D-NC noticeably deviate from 180°, whereas that for D-NB are substantially larger and closer to 180°. As a result, AFM superexchange interaction is favored in O-NB and D-NC systems, while FM double exchange interaction favored in D-NB compound between the spins of two nearest neighbor Mn ions following the Goodenough-Kanamori rule.[11] Hence, magnetic interactions strongly correlate with structural parameters, changes with *A*-site disorder as well as *A*-site cationic size mismatch of the systems.

Figures 2(d)–(f) shows magnetoresistance data of O-NB, D-NB and D-NC compounds at 80 K. A comparison of MR of these three samples indicates that the *A*-site disorder increases the MR of the systems to a higher value in low temperature range. However, the way the resistivity changes with the applied magnetic field differ for the two disorder systems suggests that localized spins of the samples respond to the magnetic field differently. This distinct response mechanism is driven by the different spin ordering in these systems, FM for D-NB and AFM for D-NC. The resistivity of the three compounds at the applied magnetic fields 0 T and 9 T has shown in Figs. 2(g)–(i). The figure demonstrates that at no applied magnetic fields, all three compounds are insulating. Resistivity of the disorder compounds substantially reduced near 80 K by the application of a strong magnetic field, which results in an insulator to metal-like transition. However, the ordered compound maintains its insulating state with a slight decrease of resistance under a large magnetic field application. This gives a possible explanation of the observance of large MR of disorder compounds compared to order one at low temperature range.

Figure 3(a) displays temperature variation of resistivity (ρ) data for the disorder systems with no magnetic fields. It is to be noted that both compounds show a similar types of semiconducting resistive properties. It has been observed that the resistivity of D-NC compound increases more rapidly below 260 K (T_{CO}). Vogt *et al.* has correlated this observation with the onset of charge ordering (Mn^{3+}/Mn^{4+}) in the system associated with the onset of AFM correlation[9] [see Fig. 2(c)]. However, no such discontinuity has been observed for D-NB system. In order to reveal the conduction mechanism of these disorder compounds, we have fitted the resistivity data with various theoretical models. Both the resistivity data are effectively described by the activation energy model[12] in the high-temperature region (T > 251 K for D-NB and T > 261 K for D-NC) [see Fig. 3(b)]:

$$\rho(T) = \rho_0 \exp\left(\frac{E_a}{kT}\right) \quad (1)$$

Here ρ_0 is a constant, E_a is the activation energy and k is the Boltzmann's constant. The value of Ea of D-NB and D-NC are 153.23 meV and 119.97 meV, respectively. In the high-temperature region, the larger resistivity of D-NB compared to D-NC might correspond to its higher activation energy value. When the temperature is lowered further, the thermal energy (kT) becomes sufficiently low to allow an electron to jump from the valance band to the conduction band with an energy gap E_a. As a result, deviation from the activation energy model occurs below 251 K/261 K for D-NB/D-NC. At this point, it is very worthy to note that the low temperature limit (261 K) for D-NC is close to the system's charge ordering temperature (T_{CO}). When the temperature is lower than T_{CO} ($T < T_{CO}$), the D-NC starts to transform into a deformed monoclinic crystal structure from an orthorhombic structure. As a result, the excess charge (electron/hole in Mn^{3+}/Mn^{4+}) localizes on a single atom instead of delocalizing

throughout the crystal. The localize charge and it's self-trapping distortion together form the "small polaron" in the system.[13] However, no such structural distortion has been observed in the D-NB system, which explains the inapplicability of the small polaron hopping mechanism in this system. The resistivity data of D-NC compound is well fitted by the small polaron hopping model[14] in the temperature range of 174 K–151 K [see Fig. 3(c)]. According to this mechanism, the resistivity is given by,

$$\frac{\rho}{T} = \rho_\alpha \exp\left(\frac{E_p}{kT}\right) \tag{2}$$

Where $\rho_\alpha = [k/\nu_{ph}Ne^2R^2C(1-C)]\exp(2\alpha R)$, N is the number of ion sites per unit volume, R is the average intersite spacing, C is the fraction of sites occupied by the polaron, α is the electron wave function decay constant, E_p is the activation energy for hopping and ν_{ph} is the optical phonon frequency is given by $k\theta_D/h$ $(=\nu_{ph})$ where θ_D is the Debye temperature. The values of $\theta_D/2$ are estimated from the temperature where linearity deviates in high-temperature zones. D-NC has θ_D of 302 K, and the calculated phonon frequency is 6.29 × 1012 Hz.

Further lowering the temperature (T < 250 K for D-NB and T < 150 K for D-NC), the carriers get localized by the disorder potential fluctuation due to the random distribution of Nd^{3+} and Ba^{2+}/Ca^{2+} ions. Mott's variable range hopping (VRH) mechanism[12,15] is thus suited to represent the resistivity data of the systems in such low-temperature regions [see Fig. 3(d)]. According to this mechanism, the expression of resistivity is given by

$$\rho(T) = \rho_\infty \exp\left[\left(\frac{T_0}{T}\right)^{1/4}\right] \tag{3}$$

The temperature scale T_0 can be utilized to know the localization length of electrons for a given density of states.[16] Hence, the disordered systems follow various conduction mechanisms at different temperature ranges.

IV. CONCLUSION

The role of A-site cationic disorder and their ionic size mismatch to control the physical properties of mixed valent perovskite manganite has been revealed here. For this purpose three samples, *A*-site ordered $NdBaMn_2O_6$ (O-NB), *A*-site disordered $NdBaMn_2O_6$ (D-NB) ($r_{Nd3+} - r_{Ba2+}$ = 0.34 Å) and *A*-site disordered $NdCaMn_2O_6$ (D-NC) ($r_{Nd3+} - r_{Ca2+}$ = 0.07 Å) samples have been synthesized. O-NB shows AFM transition associated with the structural transition. D-NB shows FM transition without any structural transition. Interestingly, D-NC also shows AFM transition associated with a crystallographic change in the system. The compound D-NC has *A*-site cations of similar sizes. Temperature variation of XRD and magnetic measurements indicate a strong correlation between magnetic and crystal structures for these compounds, which can be controlled by *A*-site disorder and *A*-site cationic mismatch. Resistivity analysis of the disorder systems indicates the presence of different conduction mechanisms at various temperature ranges. Due to magnetic field driven insulator-to-metal transition, the disorder compounds show three times larger magnetoresistance compared to order one at low temperature range. However, since the disorder compounds have different spin configurations, their MR varies differently with the applied magnetic field.

ACKNOWLEDGMENTS

The authors would like to acknowledge Mr. S. Panda and Prof. N. Mohapatra, Indian Institute of Technology Bhubaneswar, India, for helping in carrying out the magnetic measurement. Authors also like to acknowledge Dr. A. Schoekel for helping to perform the temperature-dependent XRD at P02.1 beam-line of PETRA III in DESY Synchrotron Centre, Germany. Department of atomic energy, government of India (DAE) is greatly acknowledged for the financial support.

AUTHOR DECLARATIONS

Conflict of Interest

The authors have no conflicts to disclose.

Author Contributions

Aisha Khatun: Conceptualization (equal); Data curation (lead); Formal analysis (lead); Investigation (lead); Visualization (lead); Writing – original draft (lead); Writing – review & editing (equal). **Payel Aich**: Conceptualization (supporting); Writing – review & editing (supporting). **D. Topwal**: Conceptualization (equal); Methodology (equal); Project administration (equal); Resources (equal); Supervision (equal); Writing – review & editing (equal).

DATA AVAILABILITY

The data that support the findings of this study are available within the article.

REFERENCES

[1] A. Sundaresan, A. Maignan, and B. Raveau, "Effect of *A*-site cation size mismatch on charge ordering and colossal magnetoresistance properties of perovskite manganites," Phys. Rev. B **56**, 5092 (1997).

[2] F. Millange, V. Caignaert, B. Domengès, B. Raveau, and E. Suard, "Order-disorder phenomena in new $LaBaMn_2O_{6-x}$ CMR perovskites. Crystal and magnetic structure," Chem. Mater. **10**, 1974–1983 (1998).

[3] D. Akahoshi, M. Uchida, Y. Tomioka, T. Arima, Y. Matsui, and Y. Tokura, "Random potential effect near the bicritical region in perovskite manganites as revealed by comparison with the ordered perovskite analogs," Phys. Rev. Lett. **90**, 177203 (2003).

[4] T. Nakajima, H. Yoshizawa, and Y. Ueda, "A-site randomness effect on structural and physical properties of Ba-based perovskite manganites," J. Phys. Soc. Jpn. **73**, 2283 (2004).

[5] H. Kawano, R. Kajimoto, H. Yoshizawa, Y. Tomioka, H. Kuwahara, and Y. Tokura, "Magnetic ordering and relation to the metal-insulator transition in $Pr_{1-x}Sr_xMnO_3$ and $Nd_{1-x}Sr_xMnO_3$ with $x \sim 1/2$," Phys. Rev. Lett. **78**, 4253 (1997).

[6] A. Schökel, M. Etter, A. Berghäuser, A. Horst, D. Lindackers, T. A. Whittle, S. Schmid, M. Acosta, M. Knapp, H. Ehrenberg, and M. Hinterstein, "Multi-analyser detector (MAD) for high-resolution and high-energy powder X-ray diffraction," Journal of Synchrotron Radiation **28**(1), 146 (2020).

[7]A.-C. Dippel, H.-P. Liermann, J. T. Delitz, P. Walter, H. Schulte-Schrepping, O. H. Seeck, and H. Franz, "Beamline P02.1 at PETRA III for high-resolution and high-energy powder diffraction," Journal of Synchrotron Radiation **22**(3), 675 (2015).
[8]S. Yamada, H. Sagayama, K. Higuchi, T. Sasaki, K. Sugimoto, and T. Arima, "Physical properties and crystal structure analysis of double-perovskite $NdBaMn_2O_6$ by using single crystals," Phys. Rev. B **95**, 035101 (2017).
[9]T. Vogt, A. K. Cheetham, R. Mahendiran, A. K. Raychaudhuri, R. Mahesh, and C. N. R. Rao, "Structural changes and related effects due to charge ordering in $Nd_{0.5}Ca_{0.5}MnO_3$," Phys. Rev. B **54**, 15303 (1996).
[10]F. Millange, S. d. Brion, and G. Chouteau, "Charge, orbital, and magnetic order in $Nd_{0.5}Ca_{0.5}MnO_3$," Phys. Rev. B **62**, 5619 (2000).
[11]S. Jana, P. Aich, P. Anil Kumar, O. K. Forslund, E. Nocerino, V. Pomjakushin, M. Månsson, Y. Sassa, P. Svedlindh, O. Karis, V. Siruguri, and S. Ray, "Revisiting Goodenough-Kanamori rules in a new series of double perovskites $LaSr_{1-x}Ca_xNiReO_6$, Scientific Reports **9**, 18296 (2019).
[12]B. I. Shklovskii and A. L. Efros, Electronic Properties of Doped Semiconductors (Springer-Verlag, Berlin, Heidelberg).
[13]G. Geneste, B. Amadon, M. Torrent, and G. Dezanneau, "DFT + U study of self-trapping, trapping, and mobility of oxygen-type hole polarons in barium stannate," Phys. Rev. B **96**, 134123 (2017).
[14]W. Khan, A. H. Naqvi, M. Gupta, S. Husain, and R. Kumar, "Small polaron hopping conduction mechanism in Fe doped $LaMnO_3$," The Journal of Chemical Phys **135**, 054501 (2011).
[15]M. Ziese and C. Srinitiwarawong, "Polaronic effects on the resistivity of manganite thin films," Phys. Rev. B **58**, 11519 (1998).
[16]M. Viret, L. Ranno, and J. M. D. Coey, "Magnetic localization in mixed-valence manganites," Phys. Rev. B **55** (1997) 8067.